

Application of 532 nm YAG-Laser Annealing to Crystallization of Amorphous Si Thin Films Deposited on Glass Substrates

Jong-Won Lee, Byung-Soo So, Haseung Chung* and Jin-Ha Hwang[†]

Dept. of Materials Science and Engineering, Hongik University

*Dept. of Mechanical and System Design Engineering, Hongik University

(Received February 12, 2008 : Accepted March 4, 2008)

Abstract A 532 nm Nd-YAG laser was applied to crystallize amorphous Si thin films in order to evaluate the applicability of a Nd-YAG laser to low-temperature polycrystalline Si technology. The irradiation of a green laser was controlled during the crystallization of amorphous Si thin films deposited onto glass substrates in a sophisticated process. Raman spectroscopy and UV-Visible spectrophotometry were employed to quantify the degree of crystallization in the Si thin films in terms of its optical transmission and vibrational characteristics. The effectiveness of the Nd-YAG laser is suggested as a feasible alternative that is capable of crystallizing the amorphous Si thin films.

Key words YAG laser, crystallization, amorphous Si, polycrystalline Si.

1. Introduction

Active-matrix liquid crystal displays (AMLCDs) possess the dominant position in flat panel displays despite of the continuous competition from powerful counterparts, e.g. plasma display panels (PDP) or active-matrix organic light-emitting diodes (AMOLEDs). The current LCDs have been fabricated using amorphous Si thin film transistor technology. Noticeably, there has been significant progress in luminescent materials and driving systems, i.e. the advent of organic electroluminescent materials and low temperature polycrystalline silicon (LTPS) thin film transistors.¹⁾ LTPS transistors offer much higher mobility ranging from 10 to 500 cm²/Vsec than that of the counterpart a-Si TFT which ranges from 0.3 to 1.0 cm²/Vsec.²⁻⁴⁾ Higher mobility offers i) reduction in materials costs through the incorporation of driver ICs onto glass substrates, ii) less weight in the display modules and iii) thinner thickness. Furthermore, the LTPS technology opens up the higher potential of a multifunction integration including the panel ASIC, memory, photodiodes, sensors, sound chips, etc. Second, the organic electroluminescent materials provide higher brightness, better color features, lower power consumption, and less weight in conjunction with LTPS transistors.

However, the commercialization of the AMOLEDs encounters the practical issues in mass production with

high yield, requiring strict transistor performances in parallel with inspection procedures. Among essential processes in LTPS technologies, there are gate dielectrics, crystallization of a-Si into p-Si, ion-doping and activation. In particular, LTPS technology has been advanced based on various crystallization techniques, e.g., solid phase crystallization, excimer laser annealing, rapid thermal annealing, metal-induced crystallization, etc.⁵⁻¹²⁾ The current research and development place their emphasis on excimer-laser annealing in spite of the high production cost and the difficulty in quality control of optical systems which are vulnerable to minor disturbance in the laser-irradiated conditions. In this work, the applicability of Nd-YAG laser to LTPS systems was attempted due to relatively low cost and simple maintenance procedure. Therefore, the 532 nm Nd-YAG laser is tested in order to crystallize the amorphous Si thin films. The crystallinity was evaluated using Raman spectroscopy and UV-Visible spectrometry with the aim to monitoring the structural change in crystallized Si thin films. The crystalline features are correlated to the energy density of the Nd-YAG laser. The implications are discussed toward the large-scale flat panel displays in conjunction with the active-matrix organic light-emitting diodes.

2. Experimental procedure

Amorphous Si thin films were deposited on the glass

[†]Corresponding author
E-Mail : jhwang@hongik.ac.kr (J. - H. Hwang)

substrates (Corning 1737) with the buffer layer of 3000Å using plasma-enhanced chemical vapor deposition (PECVD). The amorphous Si thin films were crystallized using the 532 nm Nd-YAG laser. The detailed setup of the Nd-YAG laser system is shown in Fig. 1. In our study, a frequency doubled, Q-switched Nd-YAG laser (Quantel, Brilliant, 532 nm) was used and controlled by a burst mode whose repetition rate and the number of pulses are 10Hz and 50, respectively. Frequency doubling from 1064 nm to 532 nm was obtained by using a Potassium Titanium Oxide Phosphate (KTP) crystal. The beam stability and pointing stability are less than 1.0% rms and 50 mrad respectively. The beam divergence is 0.5 mrad. The beam from the laser cavity was magnified 5 times by a beam expander and then focused on a sample through a homogenizer and focusing lens that has a 4.6 mm x 4.6 mm spot size. All the experiments were conducted at power density that ranges from 265 mJ/cm² to 352 mJ/cm². The laser-assisted annealing was performed at room temperature and in air.

The optical characteristics were acquired through UV-Visible spectrometry (UV-2450, Shimadzu, Kyoto, Japan), which ranges from 200 nm to 800 nm. The crystallinity was estimated using micro-Raman spectrometry (LabRam HR, Jobin Yvon, Villeneuve d'Ascq, France). The obtained Raman spectra were quantified as a function of structural components using a commercial peak-fitting software.

3. Results and Discussion

Fig. 2 shows the optical transmission in the UV-Visible range. The reflectivity of Si was assumed to be negligible at the wavelength of the green laser, i.e., 532 nm. The actual absorption is estimated to be 74.0%. The partial absorption can be even employed to crystallize Si thin films deposited on the glass substrates, although excimer laser annealing exploits complete absorption at the wavelength of 308 nm. The current work focuses on the

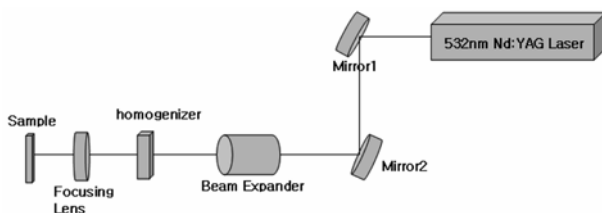


Fig. 1. Schematic diagram of a Si crystallization system incorporating an Nd : YAG laser.

applicability of Nd-YAG laser to low temperature polycrystalline Si technology. Unlike the line-scanning irradiation in commercial excimer lasing systems, the current Nd-YAG laser is illuminated onto the Si thin films in the form of the square-shaped patterns. The multiple irradiation of Nd-YAG laser changes the state of amorphous Si thin films. Fig. 3 reflects the change of Raman spectra before and after crystallization due to Nd-YAG laser irradiation. After Nd-YAG laser was irradiated onto amorphous Si thin films, noticeable changes are found in spectral shape and peak positions in Raman analysis, as can be seen in Table 1. The Raman spectral information can be analyzed in terms of degree of crystallization where the

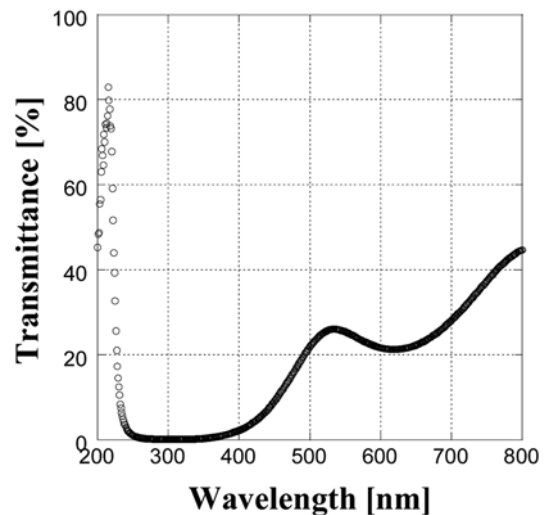


Fig. 2. UV-Visible transmission spectrum of an amorphous Si thin films as a function of wavelength.

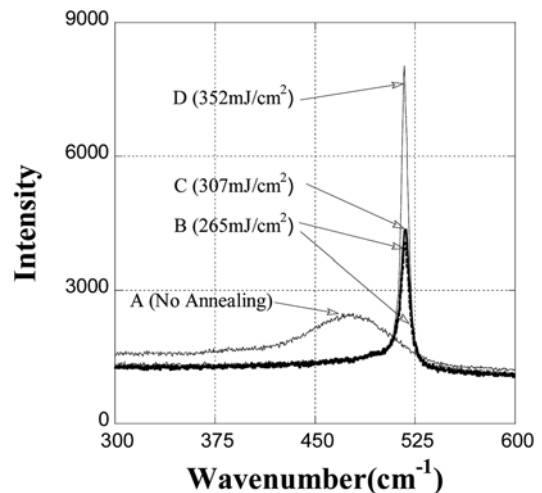


Fig. 3. Raman spectra before and after Si crystallization through an Nd : YAG laser.

Table 1. Analyzed peak fitting results for quantitative classifications, based on the raw Raman information of Fig. 3. The values in parenthesis are peak positions obtained through peak fitting

Classification	265mJ/cm ²	307 mJ/cm ²	352 mJ/cm ²
Peak I	33.1% (460.7)	29.8% (457.0)	17.6% (452.35)
Peak II	22.8% (501.55)	23% (501.67)	13.2% (495.96)
Peak III	24.5% (516.44)	26.6% (516.93)	69.2% (516.92)
Peak IV	19.6% (517.53)	20.6% (517.61)	-
Crystallized Portion (Peaks III and IV)	44.1%	47.2%	69.2%
Crystallized Portion (Corrected)*	73.8%	76.1%	88.9%

*: The crystallized portions obtained using peak deconvolution was corrected for the optical difference in amorphous and crystalline Si materials.

sophisticated modeling is required according to structural components, i.e., amorphous, defective, and crystalline Si. The Raman spectroscopy is a non-destructive tool for monitoring the characteristic of molecular vibration (or phonon in solid) that can be used for sample identification and phase quantification. The “Raman shift” is directly linked to the vibrational energy of the bonds between the atoms within the probed material.¹³⁾ The Raman analysis has been employed successfully in the quantification of the degree of crystallization in Si thin films.¹⁴⁻¹⁵⁾ In this work, the crystallized Si thin films are deconvoluted in terms of the components related to the structural issues in Si materials.

The Raman spectra were reconstructed through the Gaussian-Lorentzian distribution

$$y = 2a_0 \left[\frac{a_3 \sqrt{\ln 2}}{a_2 \sqrt{\pi}} \exp\left(-4 \ln 2 \left(\frac{x-a_1}{a_2}\right)^2\right) \frac{1-a_3}{\pi a_2 \left[1 + 4 \left(\frac{x-a_1}{a_2}\right)^2\right]} \right] \quad (1)$$

where a_0 is the area of peak, a_1 is the value of peak center, a_2 is full-width at half-maximum (FWHM), and a_3 is shape factor. The parameter a_3 varies from 0 to 1, with 0 being a pure Lorentzian and 1 being a pure Gaussian.

In Raman spectroscopy, the crystalline volume fraction (X_c) of a sample is define as:

$$X_c = \frac{V_c}{V_{\text{exp}}} \quad (2)$$

where V_c is the crystalline volume and V_{exp} is the total scattering volume in the Raman experiment for a mixed phase material (i.e. $V_{\text{exp}} = V_a + V_c$, with V_a the amorphous volume). Due to a correlation between scattering volume and the integrated Raman scattered intensities, the crystalline volume fraction of Eq. (2) can also expressed in the following manner:

$$X_c = \frac{I_c}{(I_c + yI_a)} \quad (3)$$

where I_c and I_a are the integration intensity of the crystalline and amorphous components respectively, and y is the weighting factor. The weighting factor reflects the optical difference in polycrystalline and amorphous Si thin films: the weighting factor is estimated to be 0.28. The current work suggested that the significant fractions of the several phases in poly-Si thin films can be attained through the fitting of spectrum. Usually, amorphous Si thin films exhibit the Raman shift around 480 cm^{-1} and highly-crystalline Si materials possesses the characteristic peak position of 520 cm^{-1} . Both originate from the crystalline transverse optical (TO) and amorphous TO mode. The additional Raman Shifts at 505.3 and 517.3 cm^{-1} were attributed to microcrystalline features of Si.¹⁴⁾ Comparatively, this work demonstrates that the peak deconvolution is not identical to the ideal amorphous and crystalline Si components as shown in Table 1. Additional peak contributions are required in analyzing quantitative estimation of crystallization using Nd-YAG lasers. However, the current work included another peak due to the intermediate state between amorphous and crystallized Si thin films, i.e., in nanoscale size. The interpretation is corroborated by the relative positions of the Raman shifts which are attributed to microcrystalline Si grains. Fitting accuracy was guaranteed by the confidence interval of about 99.7% throughout all fitting procedure. A typical deconvolution result is exemplified for the energy density of 352 mJ/cm^2 . (see Fig. 4).

Too high energy density of Nd-YAG laser induced ablation in amorphous Si films (not shown here). As demonstrated in Table 1 and Fig. 3, the crystalline feature is found to be noticeable above 265 mJ/cm^2 . As can be seen in Fig. 5, the amorphous fraction decreases with increasing power density and the crystalline fraction increases with power density up to 352 mJ/cm^2 . Between 265 and 352 mJ/cm^2 , the dominant peak position is located between 516 and 518 cm^{-1} . Since the peak position is quite less than that

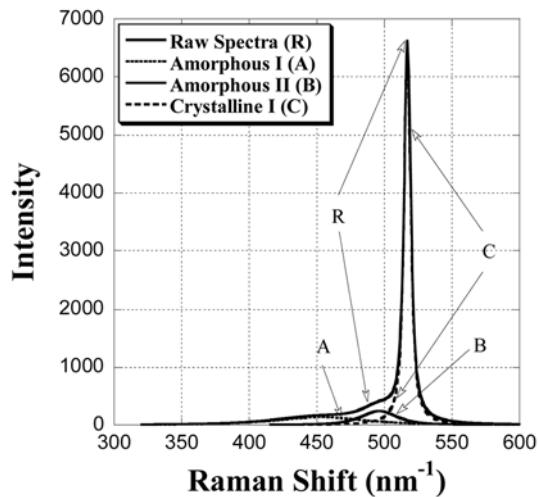


Fig. 4. A typical peak deconvolution found in the peak fitting procedure.

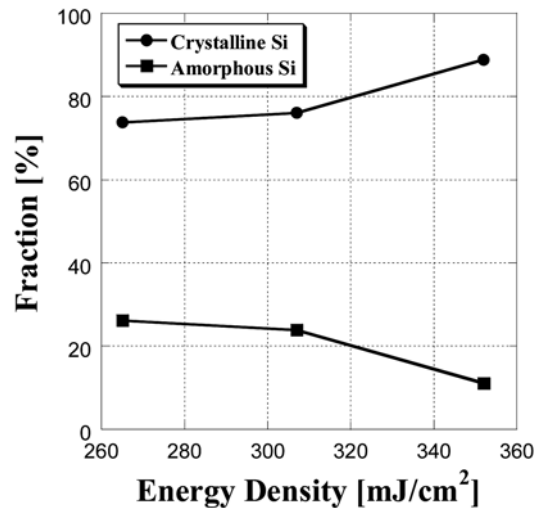


Fig. 5. Effect of energy density on Si crystallization in Nd:YAG laser annealing.

of crystalline Si (520.1 cm^{-1}), the crystalline feature appears to be related to nanoscale microstructure in grain sizes, presumably less than 50 nm. The current Nd-YAG laser can be employed in order to crystallize amorphous Si thin films, despite of the partial absorption of 532 nm laser intensity. Relatively, Nd-YAG laser annealing possesses strong advantages over the conventional excimer laser annealing, in maintenance and cost toward high yield and mass production in flat-panel applications.

Since this work reports the preliminary study on the application of Nd-YAG lasers to polycrystalline Si transistor technology, the energy distribution of the green laser within the thin layer structures and more detailed characterization in microstructure are required in the following publications.

4. Conclusions

The 532 nm Nd-YAG laser was applied in order to crystallize the amorphous Si thin films deposited on glass substrates. Depending on the energy density, the crystallized state is highly sensitive to the energy density: the optimal range is estimated to be between of 265 and 352 mJ/cm^2 , reaching even the crystallized portion of 88.9%. The applicability of Nd-YAG laser was confirmed in conjunction with the peak deconvolution approach based on Raman spectroscopy. High fraction of crystallized Si thin films implies that Nd-YAG lasers can be exploited in order to fabricate high-performance polycrystalline Si transistors.

References

1. N. Komiya, R. Nishikawa, M. Okuyama, T. Yamada, Y. Saito, S. Oima, K. Yoneda, H. Kanno, H. Takahashi, G. Rajeswaran, M. Itoh, M. Boroson and T. K. Hataer, Proceeding of the 10th International Workshop on Inorganic and Organic Electroluminescence (2000) p. 347.
2. K. Sera, F. Okumura, H. Uchida, S. Itoh, S. Karelso, and K. Hotta, IEEE Trans. Electron Devices, **36**(12), 2868 (1999).
3. M. A. Crowder, P. G. Garey, P. M. Smith, R. S. Sposili, H. S. Cho, and J. S. Im, IEEE Electron Device Lett., **19**(8), 306 (1998).
4. M. Yamamoto, H. Nishitani, M. Sakai, M. Gotoh, Y. Taketomi, T. Tsutsu, and M. Nishitani, Euro Display 99 Proceedings (1999) p.53.
5. E. Ibok and S. Garg, J. Electrochem. Soc., **140**, 2927 (1993).
6. T. W. Little, K.-I. Takahara, H. Koike, T. Nakazawa, I. Yudasaka and H. Ohshima, Jpn. J. Appl. Phys., **30**, 3724 (1991).
7. J. S. Im and R.S. Sposili, Mater. Res. Bull., **2**(3), 39 (1996).
8. R. Kakkad, J. Smith, W. S. Lau, S. J. Fonash, and R. Kerns, J. Appl. Phys., **65**, 2069 (1989).
9. O. Nast and S. R. Wenham, J. Appl. Phys., **88**, 124 (2000).
10. S. W. Lee, and S. K. Joo, IEEE Electron Device Lett., **17**(4), 160 (1996).
11. Z.Jin, G.A. Bhat, M. Yeung, H. S. Kwok, and M. Wong, J. Appl. Phys., **84**, 194 (1998).
12. S.-. Park, S.-I. Jun, K.-S. Song, C.-K. Kim and D.-K. Choi, Jpn. J. Appl. Phys., **38**, L108 (1999).
13. Vibrational Spectroscopies and NMR., Chap 8. in, Encyclopedia of Materials Characterization: Surfaces, Interfaces, Thin Films, Edited by C.R. Brundle, C.A. Evans, Jr, and S. Wilson, Manning Publishing Co., (1992) p. 413.
14. L. Tay, D.J. Lockwood, J.-M. Baribeau, X. Wu, and G.I. Sproule, J. Vac. Sci. Technol. A, **22**, 943 (2004).
15. J. Zi, H. Büscher, C. Falter, W. Ludwig, K. Zhang, and X. Xie, Appl. Phys. Lett., **69**, 200 (1996).